

See discussions, stats, and author profiles for this publication at: <https://www.researchgate.net/publication/24443799>

Reactivity and Regioselectivity in 1,3-Dipolar Cycloadditions of Azides to Strained Alkynes and Alkenes: A Computational Study

ARTICLE *in* JOURNAL OF THE AMERICAN CHEMICAL SOCIETY · JUNE 2009

Impact Factor: 12.11 · DOI: 10.1021/ja9003624 · Source: PubMed

CITATIONS

95

READS

61

4 AUTHORS, INCLUDING:



Gavin O Jones

IBM

31 PUBLICATIONS 935 CITATIONS

SEE PROFILE

Reactivity and Regioselectivity in 1,3-Dipolar Cycloadditions of Azides to Strained Alkynes and Alkenes: A Computational Study

Franziska Schoenebeck, Daniel H. Ess, Gavin O. Jones, and K. N. Houk*

*Department of Chemistry and Biochemistry, University of California,
Los Angeles, California 90095*

Received January 17, 2009; E-mail: houk@chem.ucla.edu

Abstract: The transition states and activation barriers of the 1,3-dipolar cycloadditions of azides with cycloalkynes and cycloalkenes were explored using B3LYP density functional theory (DFT) and spin component scaled SCS-MP2 methods. A survey of benzyl azide cycloadditions to substituted cyclooctynes (OMe, Cl, F, CN) showed that fluorine substitution has the most dramatic effect on reactivity. Azide cycloadditions to 3-substituted cyclooctynes prefer 1,5-addition regiochemistry in the gas phase, but CPCM solvation abolishes the regioselectivity preference, in accord with experiments in solution. The activation energies for phenyl azide addition to cycloalkynes decrease considerably as the ring size is decreased (cyclononyne $\Delta G^\ddagger = 29.2$ kcal/mol, cyclohexyne $\Delta G^\ddagger = 14.1$ kcal/mol). The origin of this trend is explained by the distortion/interaction model. Cycloalkynes are predicted to be significantly more reactive dipolarophiles than cycloalkenes. The activation barriers for the cycloadditions of phenyl azide and picryl azide (2,4,6-trinitrophenyl azide) to five- through nine-membered cycloalkenes were also studied and compared to experiment. Picryl azide has considerably lower activation barriers than phenyl azide. Dissection of the transition state energies into distortion and interaction energies revealed that “strain-promoted” cycloalkyne and cycloalkene cycloaddition transition states must still pay an energetic penalty to achieve their transition state geometries, and the differences in reactivity are more closely related to differences in distortion energies than the amount of strain released in the product. Trans-cycloalkene dipolarophiles have much lower barriers than *cis*-cycloalkenes.

1. Introduction and Background

The 1,3-dipolar cycloaddition of azides to alkynes has become one of the most important chemical ligation methods in biology and materials chemistry.¹ To “click it” has come to mean a 1,3-dipolar cycloaddition of an azide and a terminal alkyne, even though Sharpless defined click chemistry more generally.² Our group has developed a general understanding of these cycloaddition reactions over the past four decades.³ Recently, we have proposed that the energy to distort 1,3-dipoles and dipolarophiles to their transition state geometries, rather than the energy of reaction, is related to the activation energies for these reactions.⁴ For the highly reactive cyclooctyne and 3,3-difluorocyclooctyne dipolarophiles, we recently showed that distortion energy, rather than strain relief, is responsible for the fast coupling of these alkynes to azides.⁵ We now report a general investigation of

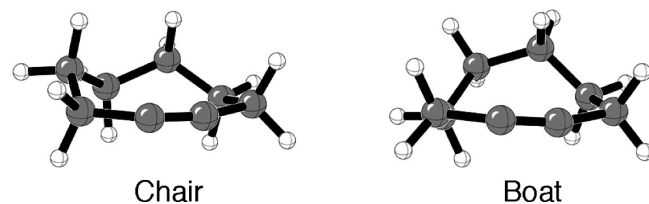


Figure 1. Chair and boat cyclooctyne.

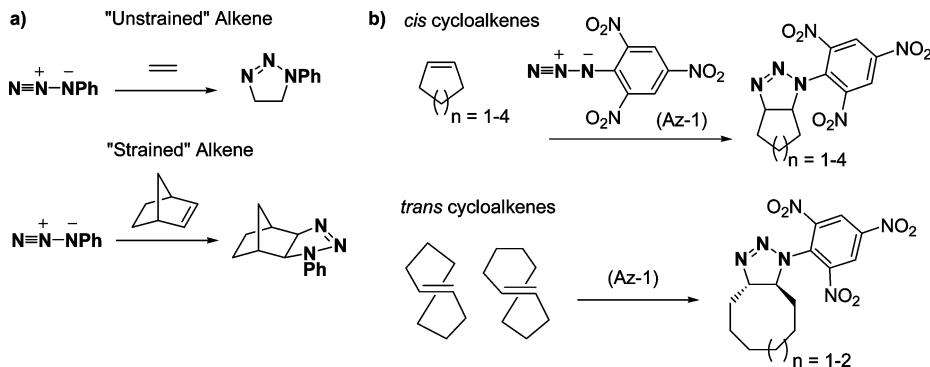
reactivity and regioselectivity for azide cycloaddition to cycloalkynes, especially cyclooctyne, and cycloalkene dipolarophiles.

Strained cyclic alkenes and alkynes often have high reactivity in cycloaddition reactions.⁶ Alder⁷ first noted that norbornene is more reactive toward phenyl azide than acyclic alkenes (Scheme 1a), and Huisgen⁸ found a greater than 10² acceleration.^{9,10} Houk and co-workers showed that this anomalously high norbornene reactivity, Huisgen’s so-called “factor

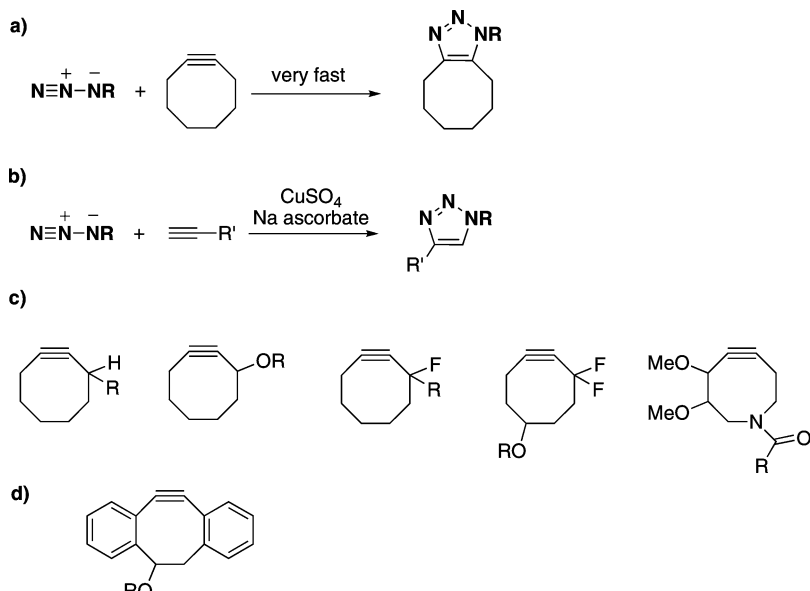
- (1) Laughlin, S. T.; Baskin, J. M.; Amacher, S. L.; Bertozzi, C. R. *Science* **2008**, *320*, 664.
- (2) Kolb, H. C.; Finn, M. G.; Sharpless, K. B. *Angew. Chem., Int. Ed.* **2001**, *40*, 2004–2021.
- (3) (a) Houk, K. N. *1,3-Dipolar Cycloaddition Chemistry*; Padwa, A., Ed.; John Wiley & Sons: New York, 1984; Vol. 2. (b) Houk, K. N.; Sims, J.; Duke, R. E., Jr.; Strozier, R. W.; George, J. K. *J. Am. Chem. Soc.* **1973**, *95*, 7287. (c) Houk, K. N.; Sims, J.; Watts, C. R.; Luskus, L. J. *J. Am. Chem. Soc.* **1973**, *95*, 7301. (d) Houk, K. N. *Acc. Chem. Res.* **1975**, *8*, 361.
- (4) (a) Ess, D. H.; Houk, K. N. *J. Am. Chem. Soc.* **2007**, *129*, 10646. (b) Ess, D. H.; Houk, K. N. *J. Am. Chem. Soc.* **2008**, *130*, 10187.
- (5) Ess, D. H.; Jones, G. O.; Houk, K. N. *Org. Lett.* **2008**, *10*, 1633.

- (6) (a) Magee, W. L.; Rao, C. B.; Glinka, J.; Hui, H.; Amick, T. J.; Fiscus, D.; Kakodkar, S.; Nair, M.; Shechter, H. *J. Org. Chem.* **1987**, *52*, 5538. (b) Palacios, F.; Heredia, I. P.; Rubiales, G. *Tetrahedron Lett.* **1993**, *34*, 4377. (c) Adam, W. *J. Am. Chem. Soc.* **1998**, *120*, 4861. (d) Adam, W.; Fröhling, B. *Org. Lett.* **2000**, *2*, 2519. (e) Becker, K. B.; Hoermuth, M. K. *Helv. Chim. Acta* **1979**, *62*, 2025. (f) Khuong, K. S.; Beaudry, C.; Trauner, D.; Houk, K. N. *J. Am. Chem. Soc.* **2005**, *127*, 3688. (g) Haddon, R. C. *J. Am. Chem. Soc.* **1987**, *109*, 1676.
- (7) (a) Alder, K.; Stein, G. *Liebigs Ann. Chem.* **1931**, 485, 211. (b) Alder, K.; Stein, G. *Liebigs Ann. Chem.* **1933**, 501, 1.

Scheme 1. (a) Examples of Unstrained and Strained Azide 1,3-Dipolar Cycloadditions and (b) Torsionally Strained Cycloalkene 1,3-Dipolar Cycloadditions Studied by Shea and Kim



Scheme 2. (a) Wittig and Krebs Cyclooctyne Cycloaddition, (b) Sharpless “Click” Cycloaddition, (c) Bertozzi Dipolarophiles, and (d) Boons Dipolarophiles



X,”⁸ is related to torsional effects,¹¹ rather than the disproportionate amount of HOMO density on the external π -face.¹² Shea and Kim have more recently studied the reactivity of torsionally strained cis and trans cycloalkenes toward picryl azide (2,4,6-trinitrophenyl azide, Scheme 1b).¹³ Based on estimations of steric energy between the alkenes and their corresponding triazolines, they concluded that “strain relief in the transition state”, rather than differences in alkene ionization potentials, is the major factor that differentiates reactivity of cycloalkene dipolarophiles.

- (8) (a) Huisgen, R.; Ooms, P. H. J.; Mingin, M.; Allinger, N. L. *J. Am. Chem. Soc.* **1980**, *102*, 3951. (b) Huisgen, R. *Pure Appl. Chem.* **1981**, *53*, 171. (c) Huisgen, R. *Angew. Chem., Int. Ed. Engl.* **1963**, *2*, 565; Huisgen, R. *Angew. Chem., Int. Ed. Engl.* **1963**, *2*, 633. (d) Huisgen, R. *Angew. Chem., Int. Ed. Engl.* **1968**, *7*, 321. (e) Huisgen, R. *1,3-Dipolar Cycloaddition Chemistry*; Padwa, A., Ed.; John Wiley & Sons: New York, 1984; Vol. 1.
- (9) (a) Wiberg, K. B.; Buergermaier, G. J.; Warner, P. *J. Am. Chem. Soc.* **1971**, *93*, 246. (b) Hrovat, D. A.; Borden, W. T. *J. Am. Chem. Soc.* **1988**, *110*, 4710. (c) Rasul, G.; Olah, G. A.; Prakash, G. K. S. *J. Phys. Chem. A* **2006**, *110*, 7197. (d) Sauers, R. R.; Harris, J. S. *J. Org. Chem.* **2001**, *66*, 7951.
- (10) Wagner, H.-U.; Szeimies, G.; Chandrasekhar, J.; Schleyer, P. v. R.; Pople, J. A.; Binkley, J. S. *J. Am. Chem. Soc.* **1978**, *100*, 1210.
- (11) Rondan, N. G.; Paddon-Row, M. N.; Caramalla, P.; Mareda, J.; Mueller, P. H.; Houk, K. N. *J. Am. Chem. Soc.* **1982**, *104*, 4974.
- (12) Inagaki, S.; Fujimoto, H.; Fukui, K. *J. Am. Chem. Soc.* **1976**, *98*, 4054.
- (13) Shea, K. J.; Kim, J.-S. *J. Am. Chem. Soc.* **1992**, *114*, 4846.

Strained C–C triple bonds also have extraordinarily high reactivity toward azides. In 1961, Krebs and Wittig showed that cyclooctyne reacts quantitatively with phenyl azide (Scheme 2a).¹⁴ Recently, Bertozzi and co-workers have developed this biologically inert reaction as an attractive alternative to the Sharpless copper-catalyzed “click” cycloaddition (Scheme 2b) for use in living systems.¹⁵ Of the five different types of cyclooctynes reported by Bertozzi (Scheme 2c), difluorocyclooctyne¹⁶ is the most reactive and has recently been used to, among many things, image glycans of developing zebrafish.¹ Boons and co-workers have also reported highly reactive

- (14) Wittig, G.; Krebs, A. *Chem. Ber.* **1961**, *94*, 3260.
- (15) (a) Laughlin, S. T.; Agard, N. J.; Baskin, J. M.; Carrico, I. S.; Chang, P. V.; Anjali, S.; Hangauer, M. J.; Lo, A.; Prescher, J. A.; Bertozzi, C. R. *Methods Enzymol.* **2006**, *415*, 230. (b) Paulick, M. G.; Forstner, M. B.; Groves, J. T.; Bertozzi, C. R. *Proc. Natl. Acad. Sci. U.S.A.* **2007**, *104*, 20332. (c) Chang, P. V.; Prescher, J. A.; Hangauer, M. J.; Bertozzi, C. R. *J. Am. Chem. Soc.* **2007**, *129*, 8400. (d) Baskin, J. M.; Bertozzi, C. R. *QSAR Comb. Sci.* **2007**, *26*, 1211. (e) Paulick, M. G.; Bertozzi, C. R. *Biochemistry* **2008**, *47*, 6991. (f) Sletten, E. M.; Bertozzi, C. R. *Org. Lett.* **2008**, *10*, 3097.
- (16) (a) Agard, N. J.; Prescher, J. A.; Bertozzi, C. R. *J. Am. Chem. Soc.* **2004**, *126*, 15046. (b) Baskin, J. M.; Preschner, J. A.; Laughlin, S. T.; Agard, N. J.; Chang, P. V.; Miller, I. A.; Lo, A.; Codelli, J. A.; Bertozzi, C. R. *Proc. Natl. Acad. Sci. U.S.A.* **2007**, *104*, 16793. (c) Agard, N. J.; Baskin, J. M.; Prescher, J. A.; Lo, A.; Bertozzi, C. R. *ACS Chem. Bio.* **2006**, *1*, 644.

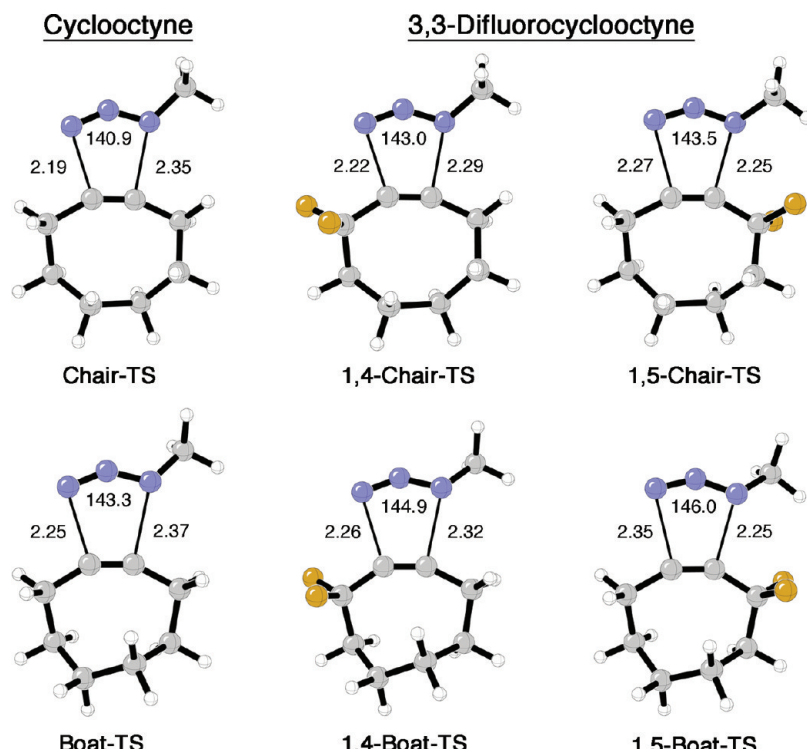


Figure 2. Chair and boat methyl azide cycloaddition transition states to cyclooctyne and 3,3-difluorocyclooctyne.

Table 1. Relative Energy Difference between Chair and Boat Transition States for the Addition of Methyl Azide to Cyclooctyne and 3,3-Difluorocyclooctyne (in kcal/mol, at 298 K)

method	cyclooctyne		3,3-difluorocyclooctyne			
	$\Delta\Delta H^\ddagger$	$\Delta\Delta G^\ddagger$	$\Delta\Delta H^\ddagger$	$\Delta\Delta G^\ddagger$	$\Delta\Delta H^\ddagger$	$\Delta\Delta G^\ddagger$
B3LYP/6-31G(d)	1.3	1.9	1.6	1.8	1.5	2.0
B3LYP/6-31+G(2d,p)	2.0	1.0	1.6	1.7	1.4	2.0
B3LYP/6-311++G(2d,p)	1.2	2.0	1.3	1.7	1.4	1.5
SCS-MP2/6-31G(d) ^a	1.0	-0.2	0.3	0.4	0.0	0.6
SCS-MP2/6-31+G(d,p) ^b	-1.3	-2.3	0.2	0.3	0.0	0.7
SCS-MP2/6-311++G(2d,p) ^c	-1.3	2.2	0.1	0.2	-0.2	0.4
CPCM (H ₂ O) B3LYP/6-31+G(d,p) ^{b,d}	-	2.2	-	1.6	-	1.6
CPCM (MeCN) B3LYP/6-31+G(d,p) ^{b,d}	-	1.1	-	2.0	-	2.0

^a B3LYP/6-31G(d) geometry. ^b B3LYP/6-31+G(d,p) geometry. ^c B3LYP/6-311++G(2d,p) geometry. ^d Radii=UAO was used.

dibenzocyclooctyne and 4-dibenzocyclooctynol analogs for glycoprotein imaging (Scheme 2d).¹⁷ To aid in the further design of facile ligation reactions, we now report a detailed study of reactivity and regioselectivity of azide cycloadditions to strained alkyne and alkene dipolarophiles.

2. Computational Methods

All gas phase B3LYP optimized stationary points were verified as minima or first-order saddle points by calculation of the full Hessian in Gaussian03.¹⁸ Solvation free energy corrections were performed using UAKS or UAO radii using B3LYP/6-31G(d) or 6-31+G(d,p) and a CPCM dielectric continuum solvent model for chloroform ($\epsilon = 4.9$) or acetonitrile ($\epsilon = 36.6$) or water ($\epsilon = 78.4$). In Table 6, CPCM (MeCN, radii=UAKS) B3LYP/6-31G(d) solvation free energy corrections were applied to the SCS-MP2/6-31G(d)/B3LYP/6-31G(d) activation free energy barriers. All

solvation free energies were converted to 1 M standard state.¹⁹ *Ab initio* spin component scaled MP2 (SCS-MP2) energies were computed on DFT geometries and also use B3LYP thermal and free energy corrections.²⁰ Fragment distortion and interaction energies were computed using B3LYP with the 6-31G(d) basis set or SCS-MP2/6-31G(d)/B3LYP/6-31G(d).

3. Results/Discussion

A. Azide–Cyclooctyne Cycloadditions. Cyclooctynes can exist in either chair or boat conformations (Figure 1).²¹ Previous work has shown the chair geometry to be more stable than the boat.²¹ For cyclooctyne and 3,3-difluorocyclooctyne, B3LYP and SCS-MP2 methods confirm that the chair geometry is preferred by 2.9 to 3.5 kcal/mol (see Supporting Information, Table S1).

(17) Ning, X.; Guo, J.; Wolfert, M. A.; Boons, G.-J. *Angew. Chem.* **2008**, *120*, 2285.

(18) Frisch, M. J.; et al. *Gaussian03*, Revision C.02; Gaussian, Inc.: Wallingford, CT, 2004. See Supporting Information for full reference.

(19) Cramer, C. J. *Essentials of Computational Chemistry, Theories and Models*, 3rd ed.; Wiley & Sons: West Sussex, England, 2004.

(20) Grimme, S. *J. Chem. Phys.* **2003**, *118*, 9095. The SCS-MP2 method scales the electron correlation energy by 6/5 and 1/3 for spin-antiparallel and spin-parallel correlation energies to reduce the overcorrection of MP2 of correlation energy.

Table 2. Activation Enthalpies, Free Energies, and Reaction Energies (given in brackets) at 298 K for the Addition of Methyl Azide to the Chair Conformer of 3,3-Difluorocyclooctyne and Cyclooctyne, Leading to the Chair Product (Energies in kcal/mol at 298 K)^a

method	cyclooctyne		1,4-addition		3,3-difluorocyclooctyne	
	ΔH^\ddagger [ΔH_{rxn}]	ΔG^\ddagger [ΔG_{rxn}]	ΔH^\ddagger [ΔH_{rxn}]	ΔG^\ddagger [ΔG_{rxn}]	ΔH^\ddagger [ΔH_{rxn}]	ΔG^\ddagger [ΔG_{rxn}]
B3LYP/6-31G(d)	10.8 [−75.5]	22.3 [−60.4]	10.0 [−75.4]	22.2 [−60.0]	7.9 [−78.3]	20.2 [−62.7]
B3LYP/6-31+G(d,p)	11.8 [−73.4]	24.8 [−58.4]	12.2 [−72.7]	24.5 [−57.4]	10.3 [−75.2]	22.5 [−59.7]
B3LYP/6-311++G(2d,p)	14.3 [−67.2]	27.3 [−52.2]	14.5 [−66.7]	26.8 [−51.5]	12.5 [−69.2]	24.8 [−53.9]
SCS-MP2/6-31G(d) ^b	12.0 [−74.6]	23.5 23.3 [−59.5]	9.2 [−74.2]	21.3 [−58.8]	6.2 [−77.8]	18.4 [−62.2]
SCS-MP2/6-31+G(d,p) ^c	12.0 [−74.9]	24.9 22.6 [−59.9]	8.7 [−74.4]	20.9 [−59.1]	6.0 [−77.5]	18.1 [−62.1]
SCS-MP2/6-311++G(2d,p) ^d	12.6 [−71.1]	25.6 23.4 [−56.1]	9.6 [−70.7]	21.8 [−55.5]	7.1 [−73.7]	19.4 [−58.3]
CPCM (H ₂ O) B3LYP/ 6-31+G(d,p) ^{c,e}	—	23.2 [−66.2]	— —	21.9 [−66.0]	— —	21.9 [−64.4]
CPCM (MeCN)	—	23.2	—	21.7	—	21.8
B3LYP/6-31+G(d,p) ^{c,e}	—	[−65.6]	—	[−63.7]	—	[−65.2]

^a Bold values correspond to the reaction path from the chair reactant to the boat transition state. ^b B3LYP/6-31G(d) geometry. ^c B3LYP/6-31+G(d,p) geometry. ^d B3LYP/6-311++G(2d,p) geometry. ^e Radii=UAO was used. Solution free energies were converted to 1 M standard state.

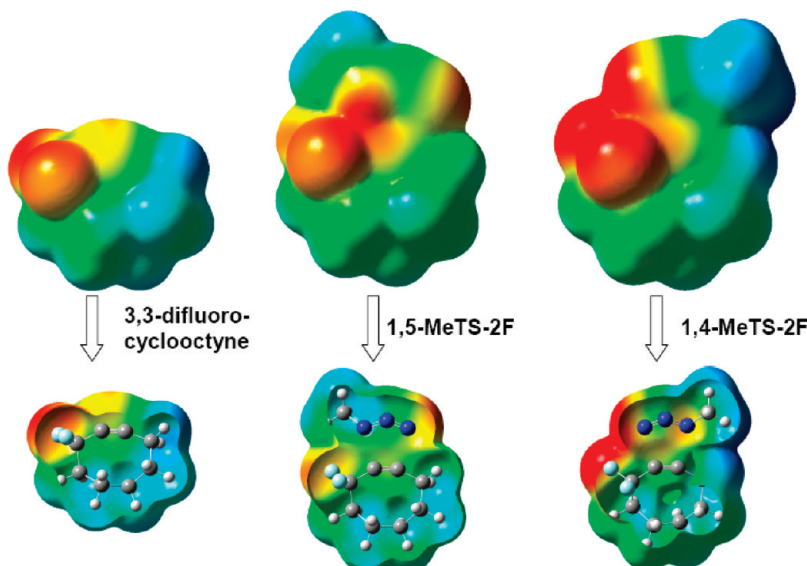


Figure 3. MP2 electrostatic potential mapped on the electron-density surface [Iso-value: 0.001] of 3,3-difluorocyclooctyne, and the 1,5 and 1,4 transition states. Color code: [−0.0425 au; +0.0425 au] with red corresponding to electron-rich and blue to electron-poor region.

Figure 2 shows the possible chair and boat cycloaddition transition states for methyl azide to cyclooctyne and 3,3-difluorocyclooctyne. The chair transition states are preferred at B3LYP level. The SCS-MP2 method with various basis sets favors the boat conformation of the transition state for the addition of methyl azide to cyclooctyne. Cycloadditions to 3,3-difluorocyclooctynes favor chair transition states with all methods (see Table 1).

As for the reactant geometries, the products are also most stable as chairs. The data is presented in the Supporting

Information (Table S2). Thus, the 1,3-dipolar cycloadditions of methyl azide to 3,3-difluorocyclooctyne involve chair conformations in the minimum energy reaction path. The addition to cyclooctyne, however, may also involve boat transition states. The corresponding activation and reaction energies are given in Table 2.

With B3LYP, increasing the basis set gives slightly larger activation barriers, as found for related reactions.²² SCS-MP2 agrees well with B3LYP/6-31G(d) and B3LYP/6-31+G(d,p). All methods reproduce the effect of fluorine substitution; even though the decrease of the activation free energy barrier compared to the cycloaddition to nonfluorinated cyclooctyne (at 298 K) is small at B3LYP. The SCS-MP2 method predicts a more pronounced lowering of activation free energy barrier

(21) (a) Yavari, I.; Nasiri, F.; Djahaniani, H.; Jabbari, A. *Int. J. Quantum Chem.* **2005**, *106*, 697. (b) Typek, V.; Haase, J.; Krebs, A. *J. Mol. Struct.* **1979**, *56*, 77. (c) Goldstein, E.; Ma, B.; Lii, J.-H.; Allinger, N. L. *J. Phys. Org. Chem.* **1996**, *9*, 191. Ring strain estimates for cyclooctyne range from 12–19 kcal/mol. See: (d) Mier, H. Cyclic Alkenes, Enynes and Dienynes. In *Advances in Strain in Organic Chemistry*; JAI Press: Greenwich, 1991, *1*, 215–272. (f) Meier, H.; Petersen, H.; Kolshorn, H. *Chem. Ber.* **1980**, *113*, 2398. (e) Detert, H.; Meier, H.; Haase, J.; Krebs, A. *Liebigs Ann. Recueil.* **1997**, *26*, 1565.

(22) (a) Ess, D. H.; Houk, K. N. *J. Phys. Chem. A* **2005**, *109*, 9542. (b) Jones, G. O.; Ess, D. H.; Houk, K. N. *Helv. Chim. Acta* **2005**, *88*, 1702. (c) Ess, D. H.; Jones, G. O.; Houk, K. N. *Adv. Synth. Catal.* **2006**, *348*, 2337.

Table 3. Activation Enthalpies, Activation Free Energies, and the Corresponding Reaction Energies (Given in Brackets) at 298 K for the Minimum Energy Reaction Pathway (Chair Reactant, Chair Transition State, Chair Cycloadduct) for Hydrazoic Acid Addition to Cyclooctyne and 3,3-Difluorocyclooctyne (in kcal/mol)

method	cyclooctyne		1,4-addition		1,5-addition	
	ΔH^\ddagger [ΔH_{rxn}]	ΔG^\ddagger [ΔG_{rxn}]	ΔH^\ddagger [ΔH_{rxn}]	ΔG^\ddagger [ΔG_{rxn}]	ΔH^\ddagger [ΔH_{rxn}]	ΔG^\ddagger [ΔG_{rxn}]
B3LYP/6-31G(d)	11.3 [-72.1]	22.2 [-57.6]	10.8 [-72.0]	22.5 [-57.4]	9.4 [-74.2]	21.3 [-59.8]
B3LYP/ 6-31+G(d,p)	12.2 [-70.2]	23.2 [-55.7]	12.6 [-69.7]	24.2 [-55.1]	11 [-72.1]	22.9 [-57.6]
B3LYP/6-311++G(2d,p)	15.1 [-63.5]	26 [-49.1]	15.2 [-63.3]	26.9 [-48.8]	13.5 [-65.6]	25.4 [-51.2]
SCS-MP2/6-31G(d) ^a	14.5 [-70.2]	25.4 [-55.7]	11.4 [-69.9]	23.1 [-55.3]	8.1 [-72.5]	20 [-58.1]
SCS-MP2/6-31+G(d,p) ^b	14.2 [-69.9]	25.2 [-55.5]	11.5 [-69.4]	23.1 [-54.9]	8 [-72.2]	19.9 [-57.7]
SCS-MP2/6-311++G(2d,p) ^c	14.9 [-65.1]	25.9 [-50.7]	12.4 [-64.8]	24.1 [-50.4]	9.3 [-67.5]	21.6 [-53.1]
CPCM (H ₂ O) B3LYP/ 6-31+G(d,p) ^{b,d}	— —	22.8 [-63.0]	— —	22.3 [-64.5]	— —	22.8 [-62.4]
CPCM (MeCN)	—	22.7	—	22.3	—	22.7
B3LYP/6-31+G(d,p) ^{b,d}	—	[-63.3]	—	[-64.2]	—	[-62.3]

^a B3LYP/6-31G(d) geometry. ^b B3LYP/6-31+G(d,p) geometry. ^c B3LYP/6-311++G(2d,p) geometry. ^d Radii=UAO was used. Solution free energies were converted to 1 M standard state.

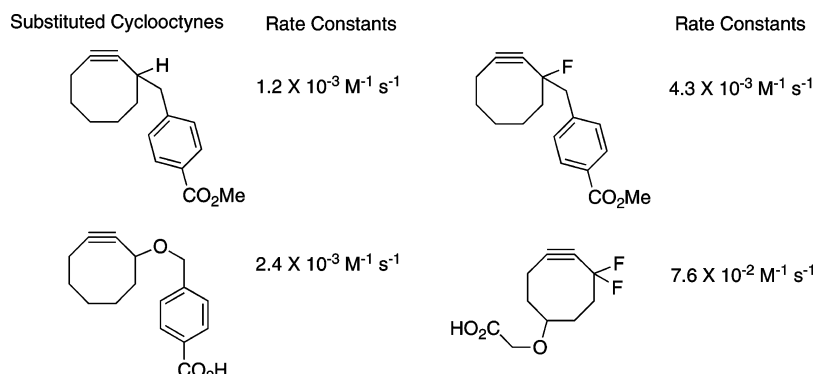


Figure 4. Benzyl azide cycloaddition rate constants reported by Bertozzi and co-workers.

upon fluorine substitution, which is in agreement with experimental findings by Bertozzi and co-workers.¹⁶

In the gas phase, regioselectivity of the cycloaddition with difluorocyclooctyne is predicted, favoring the 1,5-addition by up to 2.9 kcal/mol in activation free energy over the 1,4-configuration, depending on the method employed. Solvation free energy corrections diminish the regioselectivity, giving essentially identical activation barriers for both regioisomers. Examination of the electrostatic potential surfaces (see Figure 3) and dipoles of the 1,5- and 1,4-transition states give an explanation for this: the 1,4-isomer bears all electron-rich substituents on one side, thus exhibiting a larger dipole moment (5.5 D in gas phase, 7.0 D in water) than the 1,5-isomer (2.0 D in gas phase, 2.8 D in water); solvation hence stabilizes the 1,4-isomer more strongly than the 1,5-isomer, diminishing the gas-phase regioselectivity.

The analogous study was undertaken for the cycloaddition of hydrazoic acid to cyclooctyne and difluorocyclooctyne for chair and boat conformations. The results are given in the Supporting Information (Tables S3 and S4) and below. In this case, both B3LYP and SCS-MP2 methods predict chair conformations for reactants, transition states and products to be favored. The activation and reaction energies for the minimum energy reaction path are given in Table 3.

In contrast to the study with methyl azide, only SCS-MP2 methods are found to reflect the effect of fluorine in the free energies of activation. The 1,5-regioisomeric transition state is again predicted to be favored in the gas phase (by up to 3.0 kcal/mol) due to its lower dipole (1,4-TS: 5.1 D in gas phase; 1,5-TS: 2.8 D in gas phase); solvation corrections diminish this energy preference. That the 1,5-isomer is favored in the gas phase by a few kcal/mol (in contrast to solution) is an important observation that needs to be considered in the evaluation and future computational designs of cycloaddition systems that bear polarized substituents.

Bertozzi and co-workers have measured the second-order rate constants for benzyl azide cycloaddition to substituted cyclooctynes (Figure 4). Only difluorocyclooctyne shows a substantial increase in the reaction rate constant over cyclooctyne. Bertozzi reported that triazole regioisomers (1,5 and 1,4) are formed in a nearly equivalent ratio^{15,16} (consistent with our findings above). A similar lack of regioselective preference has also been reported for mesitonitrile cycloadditions to methoxy substituted cyclooctenes.²³ To further investigate the substituent effects, we have computed the activation barriers for benzyl azide with mono- and disubstituted cyclooctynes, using SCS-MP2/6-

(23) (a) Jendralla, H. *Tetrahedron* **1983**, *39*, 1359. (b) Berger, S.; Krebs, A.; Thölke, B.; Siehl, H.-U. *Magn. Reson. Chem.* **2000**, *38*, 566.

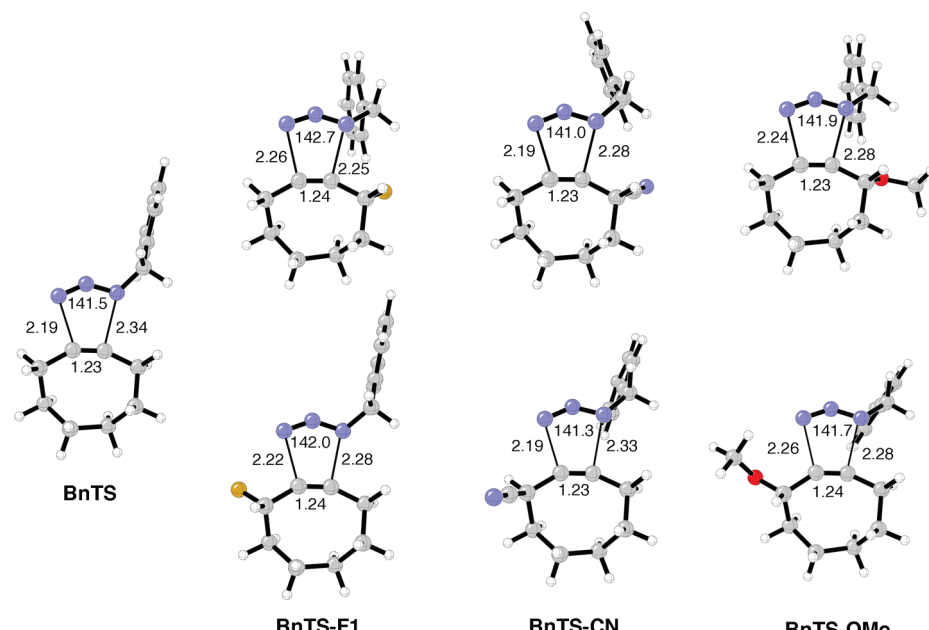


Figure 5. Monosubstituted cyclooctyne transition states.

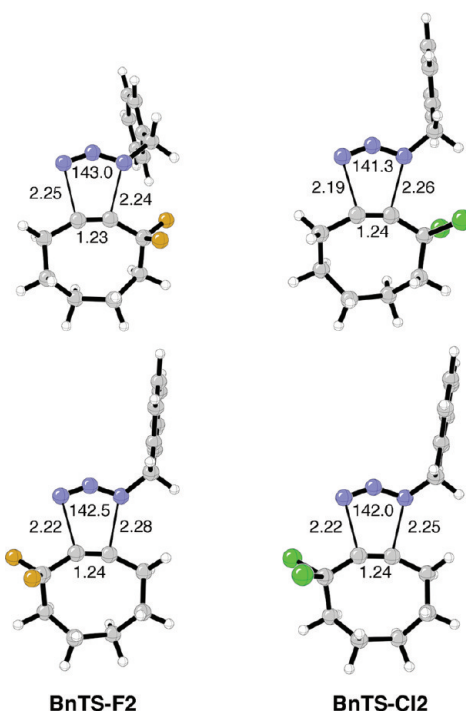


Figure 6. Disubstituted cyclooctyne transition states.

31G(d)/B3LYP/6-31G(d) that was shown above to reproduce the fluorine effect well and also showed essentially no energy difference between the boat and chair transition states. Figures 5 and 6 show the 1,5- and 1,4-addition regiosomeric cyclooctyne transition states in their chair conformations. Table 4 gives the corresponding activation barriers and free energies with acetonitrile CPCM solvation correction.

All substituents at the 3-position lower the electronic and free energy activation barriers. The gas-phase regiosiomer preference for the 1,5-regiosomeric transition state is large at SCS-MP2 (up to 6 kcal/mol electronic energy and 3 kcal/mol free energy), consistent with our findings in Table 2. Solvation free energy corrections in acetonitrile at B3LYP/6-31G(d) decrease

this preference. Since we expect the gas-phase preference of the 1,5-regiosomeric transition states to be misleading for the explanation of solution phase reactivity of substituted cyclooctynes, we focus in the following paragraph solely on the 1,4-regiosomers.

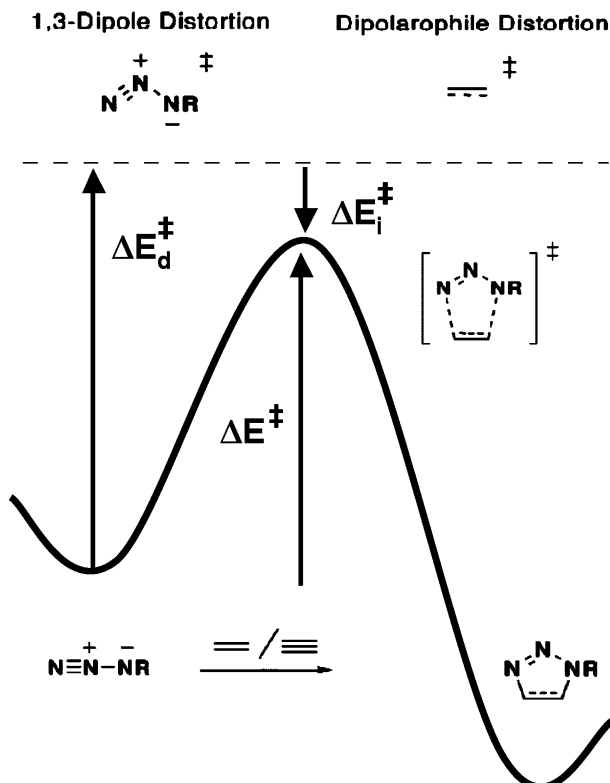
We have analyzed these substituent effects in terms of the transition state distortion and interaction energies. Previously it was shown that 1,3-dipolar cycloaddition barriers are related to the energy required to distort the 1,3-dipole and its dipolarophile counterpart into their transition state geometries (ΔE_d^\ddagger). The energy of interaction (ΔE_i^\ddagger) involves the interaction of the distorted components in the transition state geometry ($\Delta E^\ddagger = \Delta E_d^\ddagger + \Delta E_i^\ddagger$).⁴ The activation strain model of chemical reactivity, proposed by Bickelhaupt is identical to the distortion/interaction model.²⁴ Figure 7 shows a graphical display of the relationship between these quantities. When distortion energies are nearly constant across a series of reactions, then interaction energies (typically arising from electrostatic and frontier orbital interactions) control relative reactivity. The distortion energy in BnTS is computed to be 19.1 kcal/mol, of which 17.5 kcal/mol arises from the distortion of the 1,3 dipole (92%). The energy to distort cyclooctyne to its transition state geometry is small (1.7 kcal/mol), indicating its ‘predistorted’ ground-state geometry and enhanced reactivity. The 1,4-BnTS-CN and 1,4-BnTS-Cl2 show a slightly increased interaction energy (−8.9

(24) (a) Ziegler, T.; Rauk, A. *Theor. Chim. Acta* **1977**, *46*, 1. (b) Ziegler, T.; Rauk, A. *Inorg. Chem.* **1979**, *18*, 1755. (c) Bickelhaupt, F. M.; Ziegler, T.; Schleyer, P. v. R. *Organometallics* **1995**, *14*, 2288. (d) Bickelhaupt, F. M. *J. Comput. Chem.* **1999**, *20*, 114. (e) Velde, G. T.; Bickelhaupt, F. M.; Baerends, E. J.; Guerra, C. F.; Gisbergen, S. J. A. v.; Snijders, J. G.; Ziegler, T. *J. Comput. Chem.* **2001**, *22*, 931. (f) Diefenbach, A.; Bickelhaupt, F. M. *J. Chem. Phys.* **2001**, *115*, 4030. (g) Diefenbach, A.; Bickelhaupt, F. M. *J. Phys. Chem. A* **2004**, *108*, 8460. (h) Diefenbach, A.; Bickelhaupt, F. M. *J. Organomet. Chem.* **2005**, *690*, 2191. (i) Diefenbach, A.; de Jong, G. T.; Bickelhaupt, F. M. *Mol. Phys.* **2005**, *103*, 995. (j) Diefenbach, A.; de Jong, G. T.; Bickelhaupt, F. M. *J. Chem. Theory Comput.* **2005**, *1*, 286. (k) Stralen, J. N. P. v.; Bickelhaupt, F. M. *Organometallics* **2006**, *25*, 4260. (l) de Jong, G. T.; Visser, R.; Bickelhaupt, F. M. *J. Organomet. Chem.* **2006**, *691*, 4341. (m) de Jong, G. T.; Bickelhaupt, F. M. *Chem. Phys. Chem.* **2007**, *8*, 1170. (n) de Jong, G. T.; Bickelhaupt, F. M. *J. Chem. Theory Comput.* **2007**, *3*, 514.

Table 4. Activation, Distortion, Interaction, and Free Energy of Activation for Cyclooctyne Transition States (in kcal/mol), Calculated at SCS-MP2/6-31G(d)//B3LYP/6-31G(d)

	isomer	ΔE^\ddagger ^a	ΔE_d^\ddagger (dipole)	ΔE_d^\ddagger (alkyne)	ΔE_d^\ddagger (total)	ΔE_i^\ddagger	$\Delta H_{(0K)}^\ddagger$ ^a	$\Delta G_{(298K)}^\ddagger$ ^a	$\Delta G_{(298K)}^\ddagger$ ^b
BnTS		11.6	17.5	1.6	19.1	-7.5	11.9	23.2	24.9
BnTS-F1	1,5	3.8	15.4	1.8	17.2	-13.3	4.7	18.1	21.9
	1,4	10.0	15.9	1.8	17.7	-7.7	10.4	22.4	23.7
BnTS-CN	1,5	7.6	17.2	2.0	19.2	-11.7	8.1	20.8	24.7
	1,4	9.5	16.7	1.7	18.4	-8.9	9.9	21.7	23.9
BnTS-OMe	1,5	6.0	16.2	4.9	21.1	-12.8	8.2	22.2	23.9
	1,4	11.5	16.3	4.5	20.8	-12.8	12.0	24.9	24.9
BnTS-F2	1,5	4.1	15.1	1.8	16.9	-12.8	4.7	18.2	22.0
	1,4	10.2	15.4	1.8	17.2	-8.1	10.2	21.6	23.0
BnTS-Cl2	1,5	8.0	17.0	2.7	19.7	-11.6	8.5	21.0	24.9
	1,4	9.8	16.1	2.7	18.8	-8.9	10.2	22.2	24.7

^a SCS-MP2/6-31G(d)//B3LYP/6-31G(d). ^b CPCM (MeCN, radii=UAKS) B3LYP/6-31G(d) solvation free energy correction was applied to the SCS-MP2/6-31G(d)//B3LYP/6-31G(d) activation free energy barriers. Solution free energies were converted to 1 M standard state.

**Figure 7.** Relationship between activation, distortion, and interaction energies.

kcal/mol) in comparison to BnTS (-7.5 kcal/mol), while the total distortion energies are slightly decreased in comparison to BnTS. In contrast, the fluorinated examples, BnTS-F1 and BnTS-F2, have roughly the same interaction energies as BnTS (-7.7 and -8.1 kcal/mol in comparison to -7.5 kcal/mol). While the interaction energies remain nearly constant, the transition states become earlier upon increasing fluorination, which is reflected in the total distortion energy (lowered by 1.7 for monofluoro and 1.9 kcal/mol for difluoro). This decrease in distortion energy can be ascribed primarily to the major contributor, the 1,3-dipole: less distortion of the 1,3-dipole is required in order to reach the same transition state interaction energy that is present in BnTs. The decreased distortion is represented by a larger 1,3-dipole angle in Figures 5 and 6 (142.5° for 1,4-BnTS-F2 in comparison to 141.5° in BnTS). The methoxy substitution is an exception. The azide distortion energy contributes 78% to the total distortion energy, while the 3-methoxycyclooctyne distortion energy is 4.5 kcal/mol (com-

pared to 1.6 kcal/mol cyclooctyne distortion in BnTS). This increase in distortion energy is compensated by an increased interaction energy in the transition state.

To investigate the effect for fluorine substitution in more detail, we analyzed the molecular orbitals of 3,3-difluorocyclooctyne, methyl azide and the transition state fragments of the corresponding 1,4-regioisomer of the transition state. Bertozzi and co-workers have previously speculated that rate enhancement of difluorocyclooctyne versus cyclooctyne is due to lowering of the alkyne LUMO orbital. Figure 8 shows the frontier orbitals of the distorted transition state fragments of the MeTS and 1,4-MeTS-F2.²⁵ The orbital energies of the undistorted reactants are given in parentheses. If no fluorine is present (MeTS, see Figure 8a), the frontier gap between the HOMO of cyclooctyne and the LUMO of methyl azide is smallest (10.45 eV). The gap between the HOMO of N_3Me and the LUMO+1 of cyclooctyne is 11.43 eV. Fluorine substitution on cyclooctyne leads to lowering of both HOMO and LUMO. The HOMO is more strongly lowered (Figure 8b) in the ground state geometries. Distortion changes the orbital energies. The distortion of the cyclooctynes are small, and the LUMO energies are essentially unaffected by distortion. The HOMO and HOMO-1 energies are in average raised by 0.9 eV. The distortion energies of methyl azide are higher (17.5 kcal/mol for cyclooctyne and 15.4 for difluorocyclooctyne, see Table 4) than the distortion energies of cyclooctynes (1.8 for difluoro and 1.6 kcal/mol without fluorine, see Table 4), and the effect on the orbital energies is thus more pronounced.

The Mulliken charges of the transition states were analyzed using MP2/6-31G(d)//B3LYP/6-31G(d) to determine the direction and extent of charge transfer. The sum of the Mulliken charges of methyl azide in MeTS is -0.076 e, where the azide component in MeTS-F2 is nearly neutral with -0.009 e. This is in line with the smaller HOMO–LUMO gap of cyclooctyne and methyl azide in the nonfluorinated transition state, suggesting a more pronounced charge transfer from cyclooctyne to azide in that case. In addition to that, electrostatic effects between the approaching fragments in the transition are expected to alter the orbital energies, and therefore the extent of charge transfer, in particular in the presence of fluorine.

We also investigated the effect of four allylic fluorine substituents: 3,3,8,8-tetrafluorocyclooctyne would be expected

(25) (a) We use HF orbitals because Koopmans' theorem applies. See Supporting information for computed RHF/6-311++G(2d,p)//B3LYP/6-31G(d) orbital energies. (b) Janak, J. F. *Phys. Rev. B* **1978**, *18*, 7165. (c) Savin, A.; Umrigar, C. J.; Gonze, X. *Chem. Phys. Lett.* **1998**, *288*, 391.

(26) Orbital shapes are derived from HF/6-31G(d) calculation.

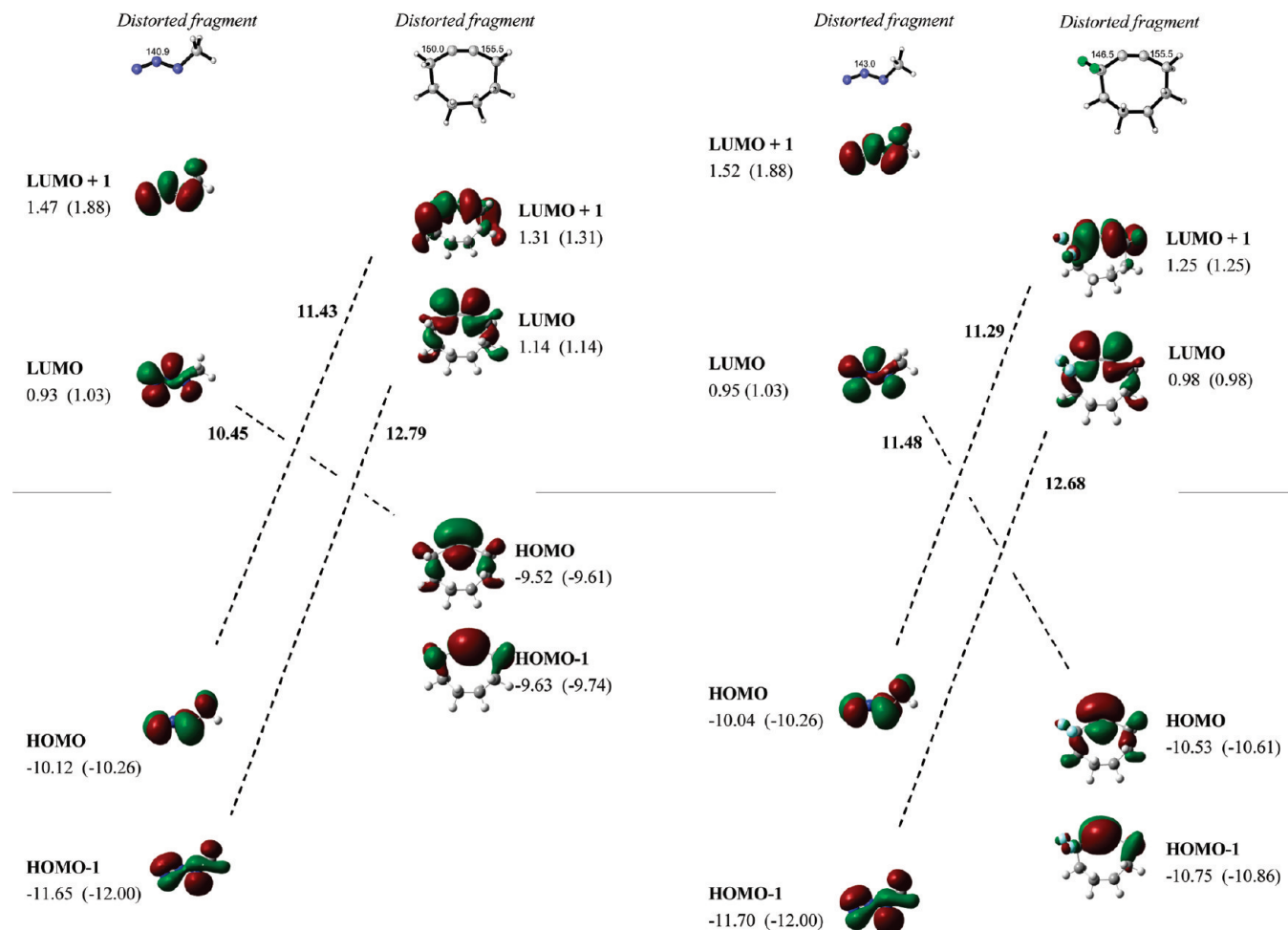


Figure 8. Distorted frontier orbital interactions (eV). Values given in parentheses are for the optimized ground state structures. Orbital energies are calculated at HF/6-311++G(2d,p).²⁶

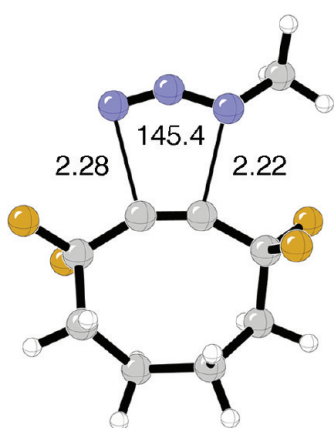


Figure 9. Transition state for the cycloaddition of methyl azide to 3,3,8,8-tetrafluorocyclooctyne.

to give rise to a partial cancellation of dipoles, and electrostatic effects in the transition state should be less pronounced. At the same time, the charge transfer from the HOMO of methyl azide to the LUMO of tetrafluorocyclooctyne should increase. Figure 9 and Table 5 give the results of the predictions for the cycloaddition of methyl azide to tetrafluorocyclooctyne.

For the cycloaddition with tetrafluorocyclooctyne, a 1.9 kcal/mol lower activation free energy barrier is predicted in water in comparison to the addition of methyl azide to difluoroc-

Table 5. Predicted Activation and Distortion Energies for the Transition State of Methyl Azide with 3,3,8,8-Tetrafluorocyclooctyne (Energies are in kcal/mol)

method	ΔE_d^\ddagger (dipole)	ΔE_d^\ddagger (alkyne)	ΔE_d^\ddagger (total)	$\Delta G_{(298)}^\ddagger$
SCS-MP2/6-31G(d) ^a	12.7	1.6	14.3	—
CPCM (H ₂ O)	—	—	—	20.9
B3LYP/6-31+G(d,p) ^{b,c}	—	—	—	19.0
B3LYP/6-31+G(2d,p)	—	—	—	19.0

^a B3LYP/6-31G(d) geometry. ^b B3LYP/6-31+G(d,p) geometry. ^c Radii=UAO was used.

cyclooctyne.²⁷ This corresponds to a ~24-fold rate acceleration. As the azide angle of 145.4° (see Figure 9) suggests, the transition state for tetrafluorocyclooctyne is even earlier than for difluorocyclooctyne. Examination of the transition state fragment orbital energies shows that, following the trend in Figure 8, the HOMO of the ground state of tetrafluorocyclooctyne is lowered even more due to the fluorine substitution (−11.6 eV, compared to −10.86 eV for difluoro and −9.74 eV for cyclooctyne). The FMO gap between the HOMO of 3,3,8,8-tetrafluorocyclooctyne and LUMO of methyl azide is increased to 12.52 eV accordingly. The gap between azide HOMO and tetrafluorocyclooctyne LUMO+1 is decreased (11.3 eV). The

(27) Chair conformations are considered.

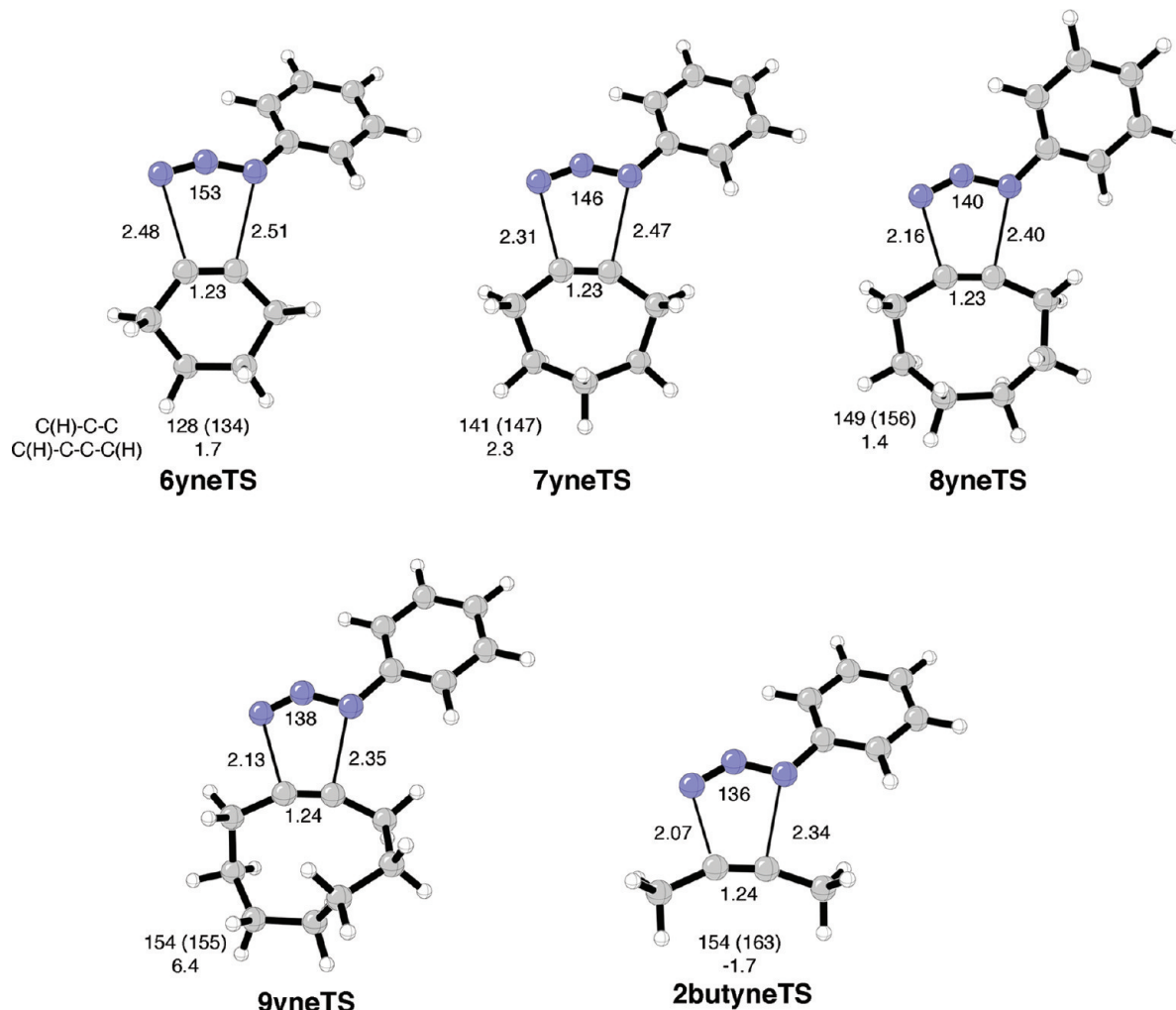


Figure 10. Lowest energy transition states for phenyl azide cycloaddition to cycloalkynes and 2-butyne.

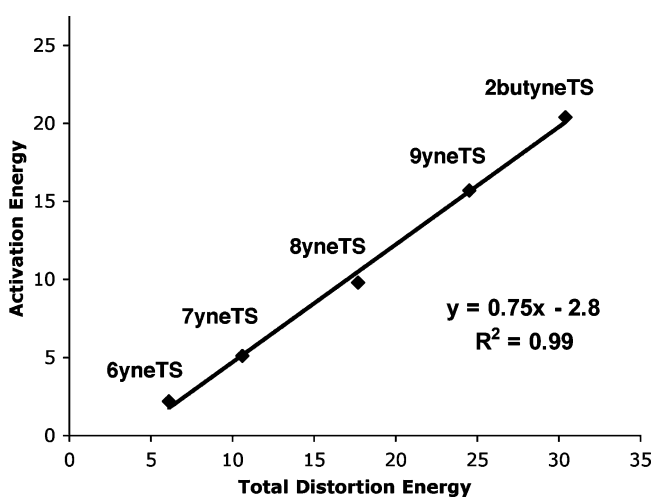


Figure 11. Correlation between activation and distortion energy for cycloalkyne transition states (energies in kcal/mol).

azide HOMO-1 vs tetrafluorocyclooctyne LUMO gap in contrast is essentially identical (12.6 eV) to difluoro case (b) in Figure 8. This suggests an improved charge transfer from the azide to tetrafluorocyclooctyne, which is in accord with the sum of the Mulliken charges of the methyl azide in the transition state, showing a large positive value of 0.342e.

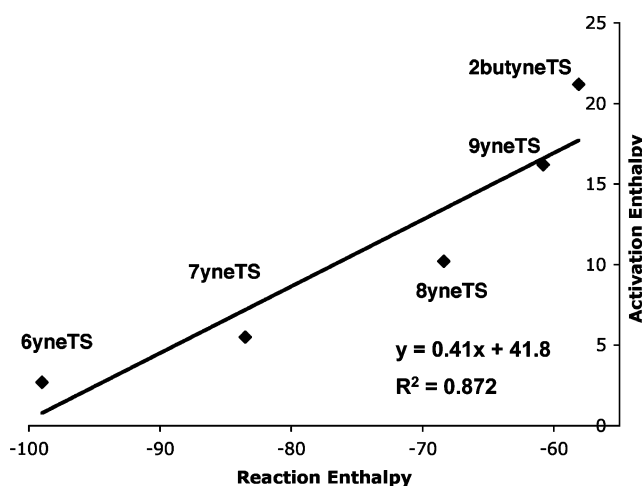


Figure 12. Correlation between activation and reaction enthalpy for cycloalkyne reactions (energies in kcal/mol).

B. Cycloadditions of Azides to Cyclohexyne, Cycloheptyne, Cyclooctyne, and Cyclononyne. Cyclopentyne is so reactive that it cycloadds to ethylene and dimerizes.²⁸ We calculate no barrier for 1,3-cycloaddition to phenyl azide. Figure 10 shows the transition states for phenyl azide cycloaddition to 2-butyne and cyclohexyne through cyclononyne. Table 6 gives the transition state activation, distortion, and interaction energies for these

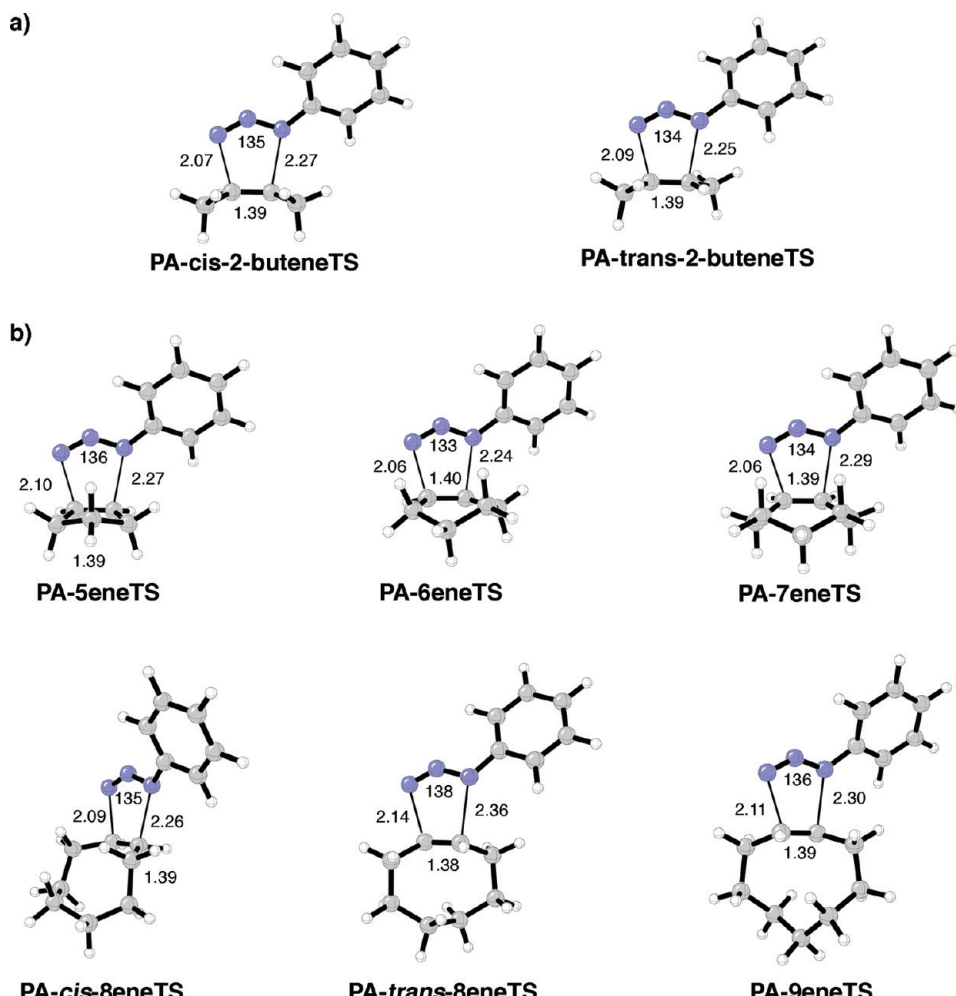


Figure 13. Transition states for phenyl azide cycloaddition to (a) *cis*- and *trans*-2-butene and (b) cycloalkenes.

Table 6. Activation, Distortion, and Interaction Energies for Transition States for Phenyl Azide with Cycloalkynes, Calculated at B3LYP/6-31G* (Energies are in kcal/mol)

	ΔE^\ddagger	$\Delta H_{(0K)}^\ddagger [\Delta H_{rxn}(0K)]$	$\Delta G_{(298K)}^\ddagger [a] [\Delta G_{rxn}(298K)]^a$	ΔE_d^\ddagger (dipole)	ΔE_d^\ddagger (alkene)	ΔE^\ddagger
6yneTS	2.2	2.7 [-99.0]	12.8 [-108.2]	5.8	0.3	-3.9
7yneTS	5.1	5.5 [-83.5]	16.0 [-91.9]	9.9	0.7	-5.5
8yneTS	9.8	10.2 [-68.4]	21.0 [-76.4]	15.5	2.2	-7.9
9yneTS	15.7	16.2 [-60.8]	27.9 [-67.3]	17.7	6.8	-8.8
2butyneTS	20.4	21.2 [-58.1]	31.1 [-51.6]	20.0	10.4	-10.0

^a Includes acetonitrile CPCM (radii=UAKS) free energy solvation corrections. Solution free energies were converted to 1 M standard state.

cycloalkyne transition states. The transition state for phenyl azide with 2-butyne, 2butyneTS, is similar to the transition state of phenylazide addition to cyclononyne, 9yneTS, with respect to both geometry and energetics (compare Table 6). This reflects the relaxed geometry and high conformational flexibility of cyclononyne.

Decreasing the cycloalkyne ring size results in an increase of distortion of the ring. Distortion energy correlates linearly with an increase in reactivity.²⁹ Thus, the transition state of the cycloaddition gets earlier with a smaller cycloalkyne ring size, corresponding to less distortion of the 1,3-dipole in the transition state geometry and less interaction between the alkyne and the 1,3-dipole. Figure 11 shows a linear relationship between the total distortion energy (dipole and alkyne) and activation energy.

The correlation is about the same as that found for the parent 1,3-dipoles reacting with ethylene and acetylene.⁴ For example, the azide component in 6yneTS has a NNN angle of 153°. This is considerably less bent than 138° in 9yneTS, which is reflected in an 11.9 kcal/mol lower distortion energy of the 1,3-dipole to

(28) (a) Gilbert, J. C.; Houk, D.-R.; Grimme, J. W. *J. Org. Chem.* **1999**, 64, 1529. (b) Gilbert, J. C.; Houk, D.-R. *J. Org. Chem.* **2003**, 68, 10067. (c) Bachrach, S. M.; Gilbert, J. C.; Laird, D. W. *J. Am. Chem. Soc.* **2001**, 123, 6706. (d) Ozkan, I.; Kinal, A. *J. Org. Chem.* **2004**, 69, 5390. (e) Bachrach, S. M.; Gilbert, J. C. *J. Org. Chem.* **2004**, 69, 6357. (f) Gilbert, J. C.; Houk, D.-R. *Tetrahedron* **2004**, 60, 469. (g) Domingo, L. R.; Pérez, P.; Contreras, R. *Eur. J. Org. Chem.* **2006**, 498. (h) Kinal, A.; Piecuch, P. *J. Phys. Chem. A* **2006**, 110, 367. (i) Leitich, J. *Tetrahedron* **1982**, 38, 1303.

(29) Taherpour, A.; Rajaeian, E. *J. Mol. Structure (THEOCHEM)* **2008**, 849, 23.

Table 7. B3LYP/6-31G(d) Activation, Distortion, and Interaction Energies for Transition States of Phenyl Azide (PA) with Alkenes and Cycloalkenes^a

	ΔE^\ddagger	$\Delta H_{(0K)}^\ddagger [\Delta H_{rxn}(0K)]$	$\Delta G_{(298K)}^\ddagger [\Delta G_{rxn}(298K)]^b$	ΔE_d^\ddagger (dipole)	ΔE_d^\ddagger (alkene)	ΔE_i^\ddagger
PA- <i>cis</i> -2-buteneTS	19.0	19.9 [20.4]	33.6 [-2.6]	22.0	8.0	-11.1
PA- <i>trans</i> -2-buteneTS	19.4	20.4 [-18.5]	34.3 [-2.9]	22.3	8.0	-10.9
PA-5eneTS	16.9	17.8 [-22.1]	32.0 [-6.1]	21.0	6.0	-10.1
PA-6eneTS	20.4	21.4 [-15.9]	35.7 [0.7]	23.4	8.4	-11.4
PA-7eneTS	17.5	18.6 [-19.4]	33.8 [-2.5]	22.0	7.1	-11.5
PA- <i>cis</i> -8eneTS	17.6	18.4 [-19.5]	32.9 [-2.5]	21.5	7.0	-10.9
PA- <i>trans</i> -8eneTS	11.3	11.9 [-29.8]	25.5 [-12.9]	17.6	2.5	-8.8
PA-9eneTS	14.0	14.9 [-22.9]	29.4 [-5.5]	20.1	3.8	-9.9

^a Reaction energies are given in brackets. Energies are in kcal/mol. ^b Includes chloroform CPCM (radii=UAKS) free energy solvation corrections. Solution free energies were converted to 1 M standard state.

Table 8. B3LYP/6-31G(d) Activation, Distortion, and Interaction Energies for Transition States of Azides with Cycloalkenes^a

	exp. ^b		computed						
	$k_{rel} (E_a)$	$\Delta \Delta G_{(298K)}^\ddagger$	$\Delta \Delta G_{(298K)}^\ddagger$	ΔE^\ddagger	$\Delta H_{(0K)}^\ddagger [\Delta H_{rxn}(0K)]$	$\Delta G_{(298K)}^\ddagger [\Delta G_{rxn}(298K)]^c$	ΔE_d^\ddagger (dipole)	ΔE_d^\ddagger (alkene)	ΔE^\ddagger
Pic- <i>cis</i> -2-buteneTS	—	—	—	12.9	14.0 [-21.3]	29.9 [-3.2]	22.5	8.0	-17.6
Pic- <i>trans</i> -2-buteneTS	—	—	—	13.4	14.4 [-21.6]	29.6 [-3.5]	22.9	8.1	-17.5
Pic-5eneTS	42	2.2	3.6	11.7	12.7 [-21.7]	27.5 [-1.9]	23.8	7.0	-19.1
Pic-6eneTS	1	0.0	0.0	15.7	16.5 [-18.1]	31.1 [1.9]	28.0	11.1	-23.8
Pic-7eneTS	53	2.3	1.7	12.1	13.1 [-19.4]	29.4 [1.0]	25.1	8.9	-21.9
Pic- <i>cis</i> -8eneTS	65 (13.3)	2.5	2.2	11.2	12.0 [-25.0]	28.9 [-3.8]	23.3	8.0	-18.9
Pic- <i>trans</i> -8eneTS	5.4×10^5 (11.2)	7.8	9.8	4.8	5.5 [-26.9]	21.3 [-6.6]	16.9	2.1	-14.2
Pic-9eneTS	1.0×10^4 (12.2)	5.5	6.0	8.2	9.1 [-21.7]	25.1 [-0.6]	19.8	9.4	-21.0

^a Reaction energies are given in brackets. Energies are in kcal/mol. ^b Kinetic parameters reported by Shea and Kim (ref 13) in CHCl_3 k_{rel} ($\text{L mol}^{-1} \text{sec}^{-1}$) at 25 °C. Solution free energies were converted to 1 M standard state. ^c Includes chloroform CPCM (radii=UAKS) free energy solvation corrections.

adopt the transition state geometry. At the same time the cyclohexyne in its reactant geometry is already very distorted, requiring only 0.3 kcal/mol energy of distortion to reach the transition state geometry. Cyclononyne in contrast requires 6.8 kcal/mol to achieve the transition state geometry.

Although the activation energies correspond to the change from early to late transition state, the correlation between enthalpy of reaction and activation enthalpy within this series is not as linear as the distortion plot (compare Figures 11 and 12), making it therefore a less powerful model for the prediction of reactivity of cycloadditions.

C. Cycloalkene Transition States. As mentioned earlier, Shea and Kim have shown that picryl azide cycloadds to strained *cis* and *trans* cycloalkenes.¹³ Very recently, Blackman et al. showed that 3,6-disubstituted tetrazines react very rapidly with *trans*-cyclooctene in an inverse electron demand cycloaddition.^{30,31} This reaction was shown to be compatible with water and rabbit lysate solution. To compare the reactivities of cycloalkene versus cycloalkyne dipolarophile reagents we have surveyed the activation barriers for phenyl azide cycloadditions to cyclopentene through cyclononene (Figure 13).³² Table 7 gives transition state activation, distortion, and interaction energies of these cycloalkene reactions.

The activation barriers for phenyl azide addition to *cis* and *trans* 2-butenes (19–20 kcal/mol) are very close to that for 2-butyne. However, cycloalkene activation barriers tend to be significantly lower than these, but higher than the corresponding cycloalkyne cycloadditions. For example, at the extreme, addition to cyclohexene requires an activation energy of 20.4

kcal/mol, while for cyclohexyne the barrier is only 2.2 kcal/mol. *Trans*-cyclooctene has a barrier that is low enough to provide facile reaction ($\Delta E^\ddagger = 11.3$ kcal/mol).

The activation barriers for these cycloalkene reactions can be understood within the distortion/interaction model. For the reactions with higher barriers, 2-butene and cyclopentene through *cis*-cyclooctene, the transition state geometries are alike; and the total distortion energies (i.e., sum of phenyl azide and alkene distortion energies) are similar, ranging from 29 to 32 kcal/mol. For *trans*-cyclooctene, the low barrier is the result of less dipole and alkene distortion energy; the transition state geometry is earlier and more asynchronous. Only about 2.5 kcal/mol is required to distort the *trans* alkene compared to 7 kcal/mol for the *cis* alkene. Cyclononene (*trans*) has a slightly higher barrier because the azide still requires 20 kcal/mol to distort, even though cyclononene requires only 4 kcal/mol to distort to the transition state geometry.

More reactive azide partners have also been studied. The nitro groups of picryl azide significantly increase the electrophilic character of this species. The experimental rates and activation barriers are given in Table 8. Figure 14 shows the transition states for cycloaddition of picryl azide to 2-butene and cycloalkenes. A comparison of phenyl azide cycloadditions (Table 7) to picryl azide (Table 8) cycloadditions shows that activation barriers are lowered by the nitro groups by an average of 8 kcal/mol. Dissection of the picryl azide activation energies into

(32) Several conformations exist for some of these alkenes and barriers for interconversion are small (<4 kcal/mol). See: (a) Allen, W. D.; Császár, A. G.; Horner, D. A. *J. Am. Chem. Soc.* **1992**, *114*, 6834. (b) Favini, G.; Buemi, G. *Raimondi J. Mol. Structure* **1968**, *2*, 137. (c) Buemi, G.; Favini, G.; Zuccarello, F. *J. Mol. Struct.* **1970**, *5*, 101. (d) Glaser, R.; Shifman, D.; Levi-Roso, G.; Ergaz, I.; Geresh, S. *J. Org. Chem.* **2002**, *67*, 5486. (e) Pawar, D. M.; Miggins, S. D.; Smith, S. V.; Noe, E. A. *J. Org. Chem.* **1999**, *64*, 2418.

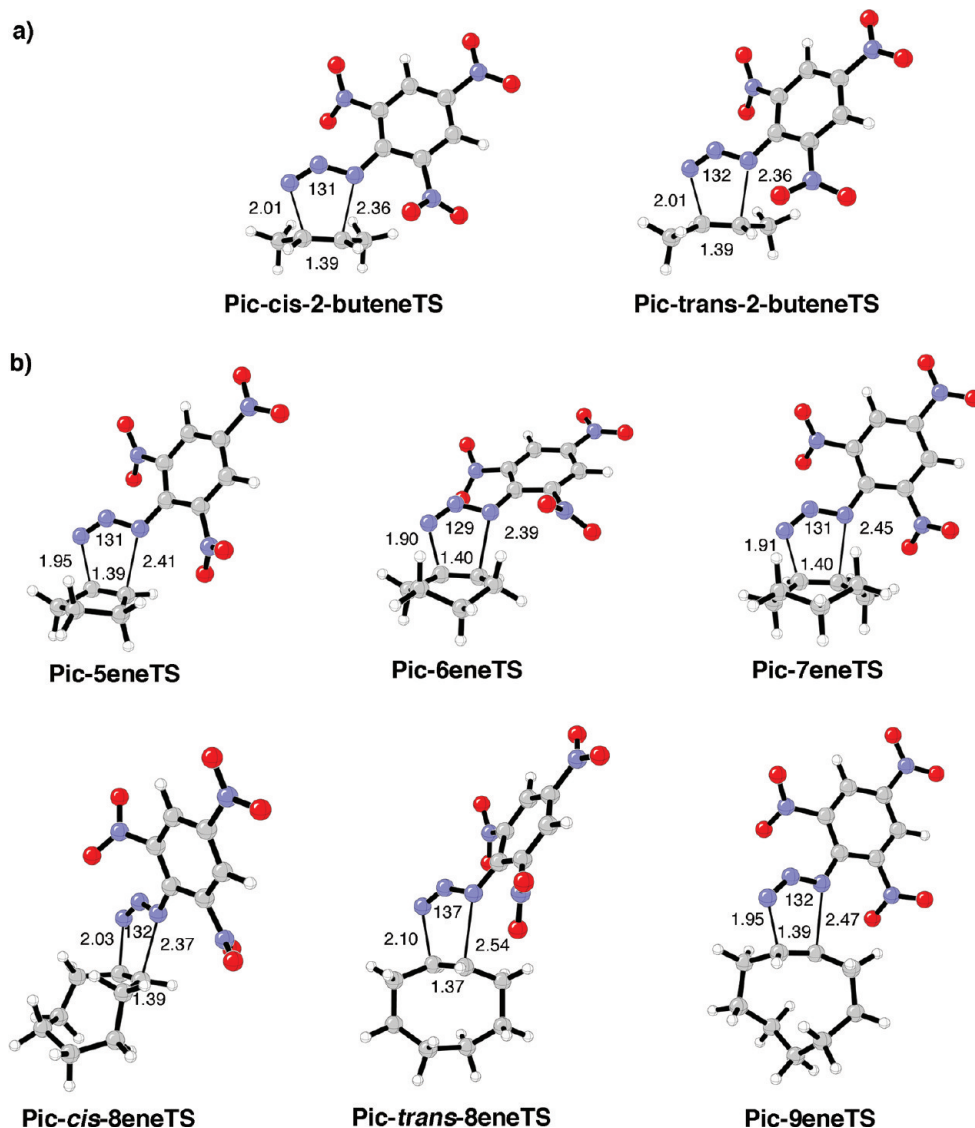


Figure 14. Transition states for picryl azide cycloaddition to (a) cis and trans 2-butene and (b) cycloalkenes.

distortion and interaction components, Table 8, reveals that nitro group substitution on the phenyl ring lowers the activation barriers by increasing the interaction energy; the picryl azide reaction distortion energies are slightly larger than phenyl azide reaction distortion energies.

The experimental relative rates measured by Shea and Kim are in rough agreement with computed solution $\Delta\Delta G^\ddagger$ values. Cyclohexene has the slowest rate of the measured cycloadditions, cyclopentene, cycloheptene and *cis*-cyclooctene have lower barriers and all react 40–65 times faster than cyclohexene. *Trans*-cyclooctene and *trans*-cyclononene have the lowest barriers and react fastest.

The results in Tables 7 and 8 show that strain released in these transition states, by transitioning from sp^2 to sp^3 hybridized carbon centers (so-called *I*-strain),³⁵ does not fully compensate for strain developed in the transition state, as measured by the alkene distortion energies. Although transition states with lower barriers typically are more exothermic, no clear correlation exists between reactivity and the energy of reaction. Cycloalkenes must

pay an energetic penalty to achieve the transition state geometry and differences in reactivity are more closely related to the differences in distortion energy, rather than alkene strain energy.³⁴ Because of the significant twisting and pyramidalization in the ground states, *trans* cycloalkenes require smaller alkene distortion energies and are more reactive toward azides. Allinger has previously discussed the different origins of strain in *cis* versus *trans* cycloalkenes.³⁵ In *cis*-cycloalkenes angle strain dominates, while in *trans*-cycloalkenes, strain is mostly due to torsion of the double bond and out-of-plane bending. Barrows and Eberlein have similarly found that most of the strain energy in *trans*-cycloalkenes is due to π -bond twisting rather than aliphatic ring interactions.³⁶

Conclusion

Exploration of reactions of azide and cyclooctynes showed that fluorine substitution most dramatically lowers the activation

(34) (a) Borden, W. T. *Chem. Rev.* **1989**, *89*, 1095. (b) Maier, W. F.; Schleyer, P.; von, R. *J. Am. Chem. Soc.* **1981**, *103*, 1891.

(35) Mastryukov, V. S.; Chen, K.-H.; Allinger, N. L. *J. Phys. Chem. A* **2001**, *105*, 8562.

(36) (a) Barrows, S. E.; Eberlein, T. H. *J. Chem. Educ.* **2005**, *82*, 1329. (b) Barrows, S. E.; Eberlein, T. H. *J. Chem. Educ.* **2005**, *82*, 1334.

(33) Eliel, E. L.; Wilen, S. H. *Stereochemistry of Organic Compounds*; John Wiley and Sons: New York, 1994; pp 769–777.

energy for cycloaddition. The 3-substituted cyclooctynes prefer 1,5-addition regiochemistry in the gas phase, but solvation nullifies the regioselectivity preference. Activation energies for azide cycloadditions to cycloalkynes decrease considerably as the ring size is decreased and have in general much lower barriers than cycloalkene dipolarophiles. Only *trans*-cyclooctene has a barrier low enough to provide facile coupling to azides at room temperature in short reaction times. However, if picryl azide is used, the barriers for addition to cycloalkenes decrease considerably. Dissection of activation energies into distortion and interaction energy components showed that so-called “strain-promoted” cycloalkene and cycloalkyne cycloaddition transition states must still pay an energetic penalty to achieve their transition state geometry. The differences between activation energies in these cases are related to differences between distortion energies.

Acknowledgment. We are grateful to the National Science Foundation and the Alexander von Humboldt Foundation (Feodor Lynen Fellowship to F.S.) for financial support. Computations were performed using the UCLA Hoffman2 cluster and the California NanoSystems Institute clusters. We thank the reviewers for their suggestions.

Supporting Information Available: Complete ref 18. B3LYP Cartesian coordinates and energies. Relative energy difference of the chair and boat 1,4- and 1,5-addition transition states of hydrazoic acid with cyclooctynes. Relative energy difference between boat and chair conformers of the products (1,4 and 1,5 regioisomers) for hydrazoic acid addition and methyl azide addition. Orbital energies and Mulliken charges. This material is available free of charge via the Internet at <http://pubs.acs.org>.

JA9003624